Diplons in the degenerate regime: exchange and correlation effects

J. Phys.: Condens. Matter **11** (1999) 6693–6706. Printed in the UK PII: S0953-8984(99)02584-9

Diplons in the degenerate regime: exchange and correlation effects

B Tanatar
Department of Physics, Bilkent University, Bilkent, 06533 Ankara, Turkey

Received 12 March 1999, in final form 12 July 1999

Abstract. We study the exchange and correlation effects on the ground-state properties of dipolar complexes (diplons) formed by the surface electrons on a liquid helium film and positive ions in the substrate supporting the helium film. We use the self-consistent-field approximation including the short-range correlations. The local-field correction, static structure function, exchange and correlation energies, and collective mode dispersions are calculated for systems with different substrates.

1. Introduction

The two-dimensional (2D) electron gas formed at the surface of liquid helium is a subject of continuing interest for several reasons [1]. Firstly, the various laws of interaction between the electrons in different experimental set-ups can be easily understood. Secondly, the density of electrons can be drastically varied by tuning the experimental parameters. For instance, the crystallization of a 2D electron system at low density is observed [2] and electrons on liquid helium are being proposed as viable systems for analogue quantum computers [3]. These interesting possibilities provide a realistic system against which many-body theories can be tested.

The 2D electron gas as formed above the surface of a liquid helium film supported by a dielectric substrate was recognized as offering possibilities for exploring the degenerate regime and has been the subject of numerous studies. Because of the stabilization of the helium film by the attractive part of the interaction between helium atoms and the substrate and the enhanced screening of the Coulomb interaction by the image charges in the substrate it becomes possible to attain the quantum regime [4, 5]. The exchange–correlation effects in a 2D electron system on a finite-thickness liquid helium film and a substrate were studied by Rino *et al* [6]. and Peeters [7] in the classical regime and by de Freitas *et al* [8] in the quantum regime. The results of these calculations have shown the importance of correctly treating the short-range correlations in describing the many-body properties. Recent experiments have started to probe the quantum regime in these systems [9, 10]. One related system is that of dipolar complexes which are called diplons. Diplons are bound dipoles made up of positive charges on an insulating substrate and electrons residing on the surface of a helium film on top of the substrate [11–13]. The system of diplons in the classical regime has been investigated by de Freitas *et al* [14]. In a recent work Cândido *et al* [15] calculated the phase diagram and Wigner crystal properties of diplons. Experimental observations of the diplon states were reported by a number of groups [16, 17]. Dahm [18] has suggested the possibility of Mott transition for the electrons bound to a lattice of positive ions beneath the helium film.

0953-8984/99/356693+14$30.00

Our aim in this work is to study the ground-state properties of diplons in the degenerate regime. As in the previous works [11, 14, 15] we assume that the positive ions on the substrate are mobile, and diplons form an interacting many-body system. We use the self-consistent-field approach of Singwi *et al* [19] (STLS) to calculate exchange–correlation effects. The STLS method has been successfully applied to a vast range of interacting electron systems [20, 21]. The correlation effects beyond the mean-field random-phase approximation (RPA) are described by a local-field correction. We further adopt the so-called sum-rule version of the STLS approach as developed by Gold [22] and Gold and Calmels [23]. which simplifies the numerical effort of solving a coupled set of nonlinear integral equations. We thus consider the various ground-state correlation functions, exchange–correlation energies, and collective mode dispersions for different substrates. Our results should be useful for experimentalists, since similar calculations can be produced with great ease for other sets of parameters. Since similar calculations were performed in the classical regime [14], our results will complement them to give a more general viewpoint.

The rest of this paper is organized as follows. We introduce the diplon interaction potential and the mean-field equations used to calculate the correlation effects in section 2. The results of our sum-rule version calculations are reported in section 3. We conclude in section 4 with a brief summary and remarks on possible extensions of our calculations.

2. Model and theory

The diplon–diplon interaction potential in the Fourier space is given by [15]

$$V(q) = \frac{2\pi e^2}{q}\left\{\delta_1[1 - \mathrm{e}^{-qd}] + \delta_2[1 - \mathrm{e}^{-2qd}]\right\} \tag{1}$$

where $\delta_1 = 4/(\epsilon_s + 1)$ and $\delta_2 = (\epsilon_s - 1)/(\epsilon_s + 1)$. Here ϵ_s is the static dielectric constant of the substrate material and we assume that the dielectric constant of the liquid helium is unity. In the subsequent calculations we consider (i) a metallic substrate with $\epsilon_s = \infty$ ($\delta_1 = 0$ and $\delta_2 = 1$), (ii) a solid-neon substrate with $\epsilon = 2$ ($\delta_1 = 4/3$ and $\delta_2 = 1/3$), and (iii) a glass substrate (sapphire) with $\epsilon_s = 10$ ($\delta_1 = 4/11$ and $\delta_2 = 9/11$). In the above interaction potential, d is the thickness of the liquid helium film, which can also be regarded as the distance between the layers of electrons and positive ions. The chief quantity characterizing the zero-temperature, degenerate electrons is the dimensionless density parameter $r_s = 1/(\pi n a_B)$, which is given in terms of the 2D electron density n, and the Bohr radius $a_B = \hbar^2/(me^2)$. In the following, we find it convenient to scale all lengths with the inverse Fermi wave vector $k_F = (2\pi n)^{1/2}$, and energies with rydbergs (Ryd $= \hbar^2/(2ma_B^2)$).

The density–density response of a many-body system for weak-to-intermediate interaction strength may be approximately expressed as

$$\chi(q, \omega) = \frac{\chi_0(q, \omega)}{1 - V(q)[1 - G(q)]\chi_0(q, \omega)} \tag{2}$$

in which $\chi_0(q, \omega)$ is the free-electron response and $G(q)$ is the local-field factor describing the exchange and short-range correlation effects beyond the RPA. The RPA is recovered by setting $G(q) = 0$. In the STLS approach the local-field correction describing the correlation effects is given by an integral over the static structure factor $S(q)$ which in turn is determined by the local-field factor. The coupled equations within the self-consistent-field approximation must be solved numerically. Similarly to the case for the other 2D electron systems [8, 24], we obtain for the diplon problem

$$G_{\mathrm{STLS}} = \frac{1}{n}\int_0^\infty \mathrm{d}k\; k[1 - S(k)]\int_0^{2\pi} \mathrm{d}\phi\; \frac{q + k\cos\phi}{(q^2 + k^2 + 2kq\cos\phi)^{1/2}}\,\frac{F(|\boldsymbol{q} + \boldsymbol{k}|)}{F(q)} \tag{3}$$

where we have defined $V(q) = (2\pi e^2/q)F(q)$. The above form of the local-field factor for the electrons on the surface of a helium film supported by a metallic substrate ($\delta_1 = 0$ and $\delta_2 = 1$) has been considered by de Freitas *et al* [8]. The static structure factor is evaluated by means of the fluctuation-dissipation theorem:

$$S(q) = -\frac{1}{n\pi}\int_0^\infty \mathrm{d}\omega\ \mathrm{Im}[\chi(q,\omega)] \tag{4}$$

which contains contributions from the single-particle excitations (electron–hole pair excitations) and the collective modes.

Rather than attempting to solve the full STLS equations numerically, we adopt the sum-rule version introduced by Gold [22]. The sum-rule approach to the STLS equations has been successfully applied to electron gas problems in various dimensions [23]. We propose the following analytical form to describe the local-field correction:

$$G(q) = \frac{C_1(r_s,d)q}{[q^2 + C_2(r_s,d)^2]^{1/2}}\frac{F([q^2 + C_2(r_s,d)^2]^{1/2})}{F(q)} \tag{5}$$

in terms of the r_s- and d-dependent parameters $C_1(r_s,d)$ and $C_2(r_s,d)$. The above form of the local-field factor is motivated by the Hubbard approximation and may be regarded as a generalized form of it. The limiting forms of $G(q)$ for long wavelengths ($q \to 0$) and as $q \to \infty$ are given by

$$G(q \to 0) = \frac{C_1(r_s,d)F(C_2(r_s,d))}{C_2(r_s,d)d(\delta_1 + 2\delta_2)} \tag{6}$$

and

$$G(q \to \infty) = C_1(r_s,d) \tag{7}$$

respectively. In obtaining the above limits we have used the fact that

$$F(q \to 0) = qd(\delta_1 + 2\delta_2).$$

Using the analytical expression for the local-field correction, and the exact STLS form $G_{\mathrm{STLS}}(q)$, we determine the coefficients $C_1(r_s,d)$ and $C_2(r_s,d)$ within the sum-rule approach by comparing the small- and large-q limits of both equation (3) and equation (5), obtaining

$$C_1(r_s,d) = \int_0^\infty \mathrm{d}k\ k[1 - S(k)] \tag{8}$$

and

$$\frac{C_1(r_s,d)F(C_2(r_s,d))}{C_2(r_s,d)} = \frac{1}{2}\int_0^\infty \mathrm{d}k\ [1 - S(k)]F(k). \tag{9}$$

Thus, our equation (5) is an interpolation formula for the STLS local-field factor constrained to reproduce the low- and high-q behaviour.

We have also found it useful to employ the following analytical form of the static structure factor:

$$S(q) = \left[1/S_0(q)^2 + 4mnV(q)[1 - G(q)]/q^2\right]^{-1/2} \tag{10}$$

which may be regarded as the generalized mean-spherical approximation. Similar forms of $S(q)$ have been used by Gold [22] and Gold and Calmels [23]. This analytical form of $S(q)$ takes the single-particle effects (through $S_0(q)$) and the collective effects (through the second term) in the above expression into account; these determine the underlying physics in different density regimes. Equation (10) can most easily be obtained within the mean-spherical approximation which replaces the noninteracting response function for fermions with that of bosons in the spirit of the plasmon-pole approximation. The power of the sum-rule approach

lies in the fact that it simplifies the self-consistent calculation of $G(q)$ and $S(q)$ based on an iterative scheme. Previous applications [22, 23] have shown that the sum-rule version faithfully reproduces the results of full STLS calculations, and we believe that it also works well in the present problem. The mean-field-approximation nature of the STLS scheme limits its applicability to very low-density systems (say, $r_s \gtrsim 20$).

3. Results

We have solved the coupled integral equations for the coefficients $C_1(r_s, d)$ and $C_2(r_s, d)$ numerically for a variety of values of the density parameter r_s and liquid helium film thickness d. Our results for metallic, solid-neon, and sapphire substrates are summarized in tables 1–3, respectively. Once the unknown coefficients in the local-field factor $G(q)$ are determined, all the physical properties of a system of interacting diplons can be calculated. We show the

Table 1. The coefficients in the local-field factor $G(q)$ for a metallic substrate.

$d = 0.1a_B$		
r_s	$C_1(r_s, d)$	$C_2(r_s, d)$
0.1	0.56728	1.85268
0.5	0.71893	4.69988
1.0	0.80437	8.10310
5.0	0.98958	33.42120
10.0	1.05592	63.72250
20.0	1.11390	122.91904
$d = a_B$		
r_s	$C_1(r_s, d)$	$C_2(r_s, d)$
0.1	0.56561	1.31629
0.5	0.74177	1.75473
1.0	0.87334	2.19544
5.0	1.16357	4.58514
10.0	1.21957	6.81926
20.0	1.24389	10.68602
$d = 10a_B$		
r_s	$C_1(r_s, d)$	$C_2(r_s, d)$
0.1	0.56519	1.26931
0.5	0.73307	1.48278
1.0	0.84775	1.60926
5.0	1.07392	1.83709
10.0	1.11771	1.94123
20.0	1.12883	2.09591
$d = 100a_B$		
r_s	$C_1(r_s, d)$	$C_2(r_s, d)$
0.1	0.56514	1.26475
0.5	0.73218	1.45857
1.0	0.84491	1.56025
5.0	1.05228	1.61786
10.0	1.08041	1.54916
20.0	1.08254	1.45894

Table 2. The coefficients in the local-field factor $G(q)$ for a solid-neon substrate ($\epsilon_s = 2$).

$d = 0.1a_B$		
r_s	$C_1(r_s, d)$	$C_2(r_s, d)$
0.1	0.60281	2.36845
0.5	0.77547	6.89243
1.0	0.85948	12.19799
5.0	1.03139	51.69671
10.0	1.09173	99.08042
20.0	1.14443	191.77890
$d = a_B$		
r_s	$C_1(r_s, d)$	$C_2(r_s, d)$
0.1	0.60286	1.40687
0.5	0.83656	2.09417
1.0	0.97881	2.74688
5.0	1.19946	6.06144
10.0	1.22994	9.20768
20.0	1.24221	14.74052
$d = 10a_B$		
r_s	$C_1(r_s, d)$	$C_2(r_s, d)$
0.1	0.60163	1.31924
0.5	0.81660	1.57988
1.0	0.93466	1.70260
5.0	1.11145	1.93824
10.0	1.12914	2.08102
20.0	1.11547	2.26326
$d = 100a_B$		
r_s	$C_1(r_s, d)$	$C_2(r_s, d)$
0.1	0.60151	1.31088
0.5	0.81430	1.53573
1.0	0.92811	1.61513
5.0	1.07646	1.57325
10.0	1.08402	1.48742
20.0	1.07675	1.40323

dependence of $G(q)$ on the helium film thickness in figure 1 for the case of a metallic substrate. For small values of d, the local-field factor has a finite value at $q \approx 0$, since the diplon–diplon interaction assumes a constant form $V(q) = 4\pi e^2 d$ as $qd \ll 1$. $G(q)$ for other substrates shows similar qualitative and quantitative behaviour to that in figure 1. It is interesting to note that the long-wavelength limit of $G(q \to 0)$ does not yield the RPA results as in the uniform electron gas systems interacting via the bare Coulomb potential. The dipolar nature of the interaction is responsible for this behaviour [8]. The static structure factor at $r_s = 10$ for a sapphire substrate is displayed in figure 2. The dotted, dashed, dot–dashed, and solid lines indicate $d = 0.1a_B$, $d = a_B$, $d = 10a_B$, and $d = 100a_B$, respectively. The thin lines show the RPA results, i.e. when $G(q) = 0$. We note that for small values of d the STLS and RPA static structure factors are rather close for this relatively low-density example ($r_s = 10$), but as d is increased the typical differences between the STLS and RPA results become clearer. We have also obtained $S(q)$ for other types of substrate and the results are qualitatively almost

Table 3. The coefficients in the local-field factor $G(q)$ for a sapphire substrate ($\epsilon_s = 10$).

$d = 0.1a_B$		
r_s	$C_1(r_s, d)$	$C_2(r_s, d)$
0.1	0.57707	2.00574
0.5	0.73406	5.23562
1.0	0.81887	9.06512
5.0	0.99995	37.51263
10.0	1.06449	71.55012
20.0	1.12089	138.03538
$d = a_B$		
r_s	$C_1(r_s, d)$	$C_2(r_s, d)$
0.1	0.57624	1.34623
0.5	0.77093	1.87207
1.0	0.90630	2.37670
5.0	1.17200	4.96195
10.0	1.21924	7.37532
20.0	1.23964	11.57061
$d = 10a_B$		
r_s	$C_1(r_s, d)$	$C_2(r_s, d)$
0.1	0.57561	1.28419
0.5	0.75938	1.51643
1.0	0.87696	1.64568
5.0	1.08955	1.88625
10.0	1.12328	2.00060
20.0	1.12398	2.15145
$d = 100a_B$		
r_s	$C_1(r_s, d)$	$C_2(r_s, d)$
0.1	0.57554	1.27819
0.5	0.75806	1.48456
1.0	0.87289	1.58153
5.0	1.06256	1.60768
10.0	1.08314	1.53272
20.0	1.08156	1.44491

the same. The most interesting feature of our $S(q)$ results based on the degenerate electron gas model is that for small values of d, $S(q)$ approaches the noninteracting case value $S_0(q)$, whereas in the classical case [6, 14] a finite value is reached as $q \to 0$.

3.1. The pair-correlation function

The probability of finding two electrons separated by a distance r is given by

$$g(r) = 1 + \int_0^\infty \mathrm{d}k\, kJ_0(kr)[S(k) - 1] \tag{11}$$

where $J_0(x)$ is the zeroth-order Bessel function. Using the analytic form of $S(q)$ with the previously determined coefficients $C_1(r_s, d)$ and $C_2(r_s, d)$ we evaluate equation (11) numerically. Figure 3 illustrates the pair-correlation function for diplons on a solid-neon substrate at $r_s = 2$ for two different helium film thicknesses (solid line: $d = 50a_B$; dashed

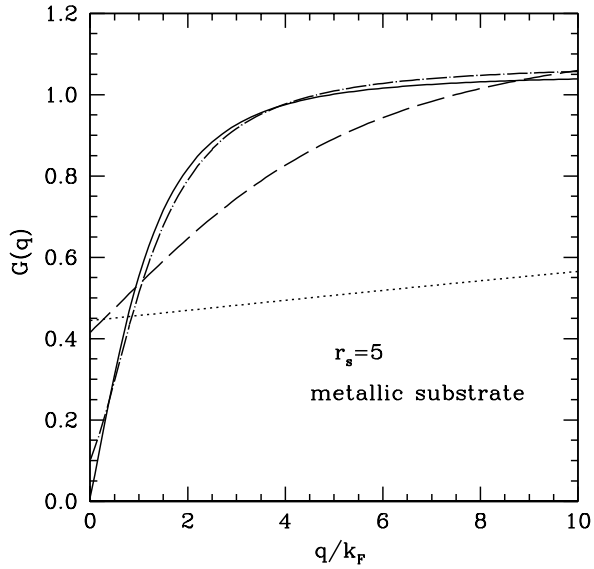

Figure 1. The local-field factor $G(q)$ at $r_s = 5$ for a metallic substrate. The dotted, dashed, dot–dashed, and solid lines indicate $d = 0.1a_B$, $d = a_B$, $d = 10a_B$, and $d = 100a_B$, respectively.

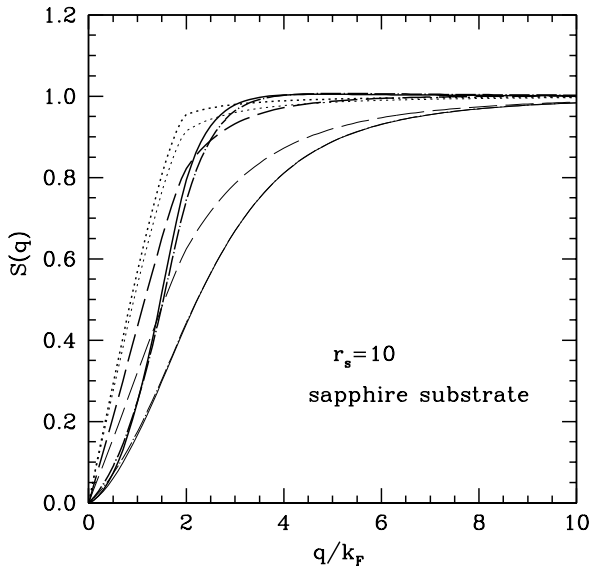

Figure 2. The static structure factor $S(q)$ at $r_s = 10$ for a sapphire substrate ($\epsilon_s = 10$). The dotted, dashed, dot–dashed, and solid lines indicate $d = 0.1a_B$, $d = a_B$, $d = 10a_B$, and $d = 100a_B$, respectively. The thick and thin lines are with and without the local-field correction.

line: $d = 10a_B$). The results for $g(r)$ in the RPA are also depicted by the thin lines. We observe that the unphysically large negative behaviour of $g(r)$ in the RPA is largely remedied when the local-field effects are taken into account. The pair-correlation function at zero separation, $g(0)$, takes a particularly simple form in our approximate scheme, $g(0) = 1 - C_1(r_s, d)$. In

figure 4 we show $g(0)$ as a function of the density parameter r_s for diplons on a neon substrate. $g(0)$ calculated in the STLS scheme, in comparison to the RPA, becomes negative at a higher r_s-value. This shows the importance of including the short-range correlation effects in the calculation of the ground-state structure.

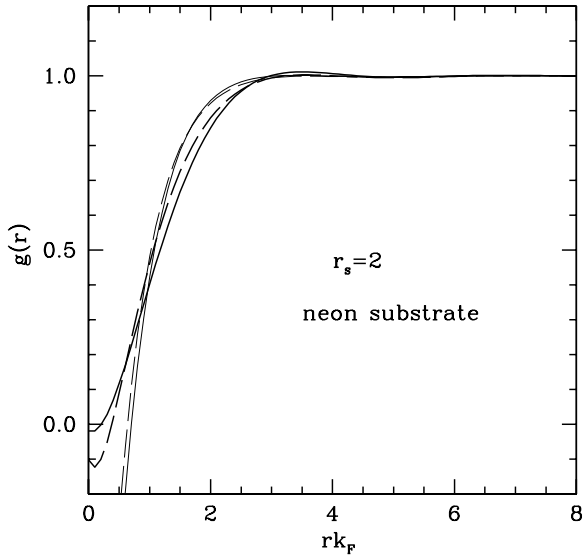

Figure 3. The pair-correlation function $g(r)$ at $r_s = 2$ for a solid-neon substrate. The solid and dashed lines indicate $d = 50a_B$ and $d = 10a_B$, respectively. The RPA results for $g(r)$ are shown by the thin lines.

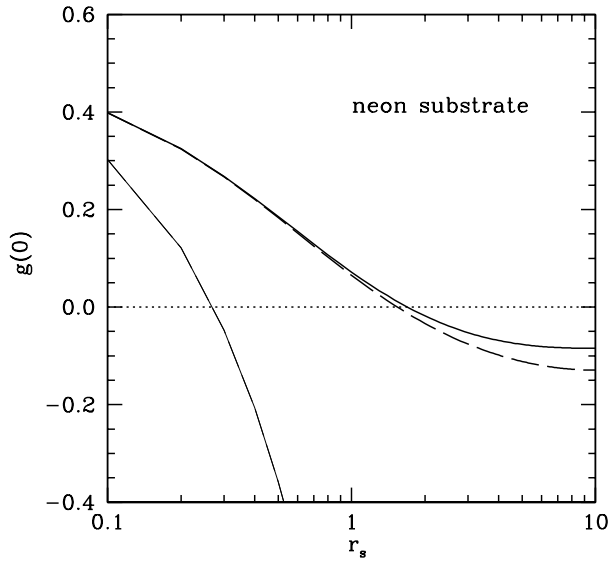

Figure 4. The pair-correlation function at zero separation $g(0)$ as a function of $r_s = 2$ for a solid-neon substrate. The solid and dashed lines indicate $d = 100a_B$ and $d = 10a_B$, respectively. The thin line is the RPA result for $g(0)$.

3.2. Exchange and correlation energies

The ground-state energy of the interacting system of diplons is written as a sum of the kinetic energy and exchange and correlation terms. The kinetic energy per particle is simply $K = 1/r_s^2$ (in units of rydbergs). The exchange energy is given by

$$E_{\rm ex} = \frac{\sqrt{2}}{r_s}\int_0^\infty {\rm d}q\ F(q)[S_0(q) - 1] \tag{12}$$

where $S_0(q)$ is the Hartree–Fock static structure factor appropriate for a noninteracting system. The exchange energy $E_{\rm ex}$ as a function of r_s is shown in figure 5. The correlation energy, on the other hand, is given by

$$E_{\rm cor} = \frac{\sqrt{2}}{r_s^2}\int_0^{r_s} {\rm d}r_s'\int_0^\infty {\rm d}q\ F(q)[S(q;r_s) - S_0(q)] \tag{13}$$

as an integral over the coupling constant. The correlation energy $E_{\rm cor}$ for diplons of the same substrate is shown in figure 6(a) for several helium film thicknesses. We observe that the correlation energy is very important in the density range of interest. The RPA (shown by thin lines) overestimates the correlation energy which is more visible for large film thicknesses. To highlight the difference between the degenerate and the classical regimes [6], we plot the correlation energy $E_{\rm cor}$ as a function of the helium film thickness for different substrates in figure 6(b). $E_{\rm cor}$ becomes negligibly small as d vanishes, because of the enhanced screening of the electrons by the substrate as in the classical case. Similarly, the correlation energy tends to different constant values (depending on the substrate) for large d. Other thermodynamic quantities of interest such as the pressure and compressibility can easily be evaluated as derivatives of the ground-state energy terms with respect to the density parameter.

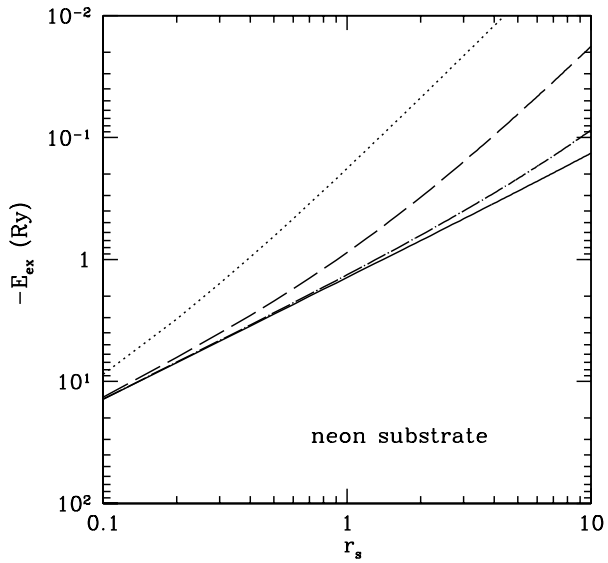

Figure 5. The exchange energy $E_{\rm ex}$ as a function of r_s for a solid-neon substrate. The dotted, dashed, dot–dashed, and solid lines indicate $d = 0.1a_B$, $d = a_B$, $d = 10a_B$, and $d = 100a_B$, respectively.

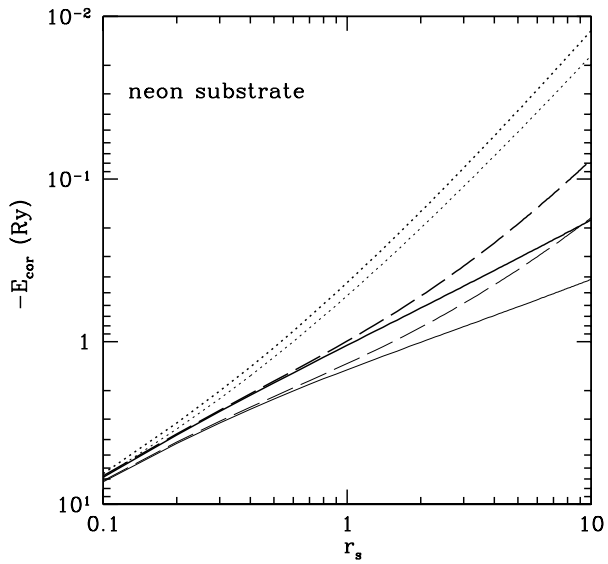

(a)

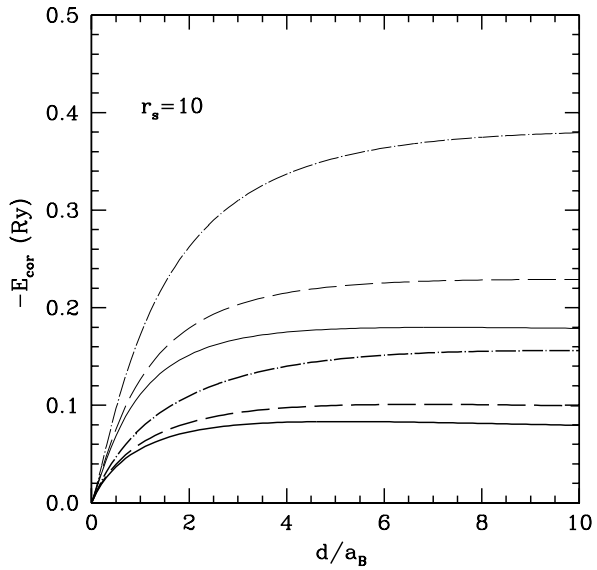

(b)

Figure 6. (a) The correlation energy $E_{\rm cor}$ as a function of r_s for a solid-neon substrate. The dotted, dashed, dot–dashed, and solid lines indicate $d = 0.1a_B$, $d = a_B$, $d = 10a_B$, and $d = 100a_B$, respectively. (b) $E_{\rm cor}$ as a function of d. The solid, dot–dashed, and dashed lines indicate metallic, solid-neon, and sapphire substrates, respectively. The STLS and RPA calculations are distinguished by the thick and thin lines respectively.

3.3. Collective excitations

The collective excitation modes of the interacting system of diplons are calculated from the zero of $1 - V(q)[1 - G(q)]\chi_0(q, \omega_{\rm pl}) = 0$, where $\chi_0(q, \omega)$ is the free-electron dynamic

susceptibility in 2D. We find that the dispersion relation for diplon plasmons is given by

$$\omega_{\rm pl}(q)/E_F = q(1+z)\left[q^2 + \frac{4}{z^2+2z}\right]^{1/2} \tag{14}$$

in which $z = q/[\sqrt{2}r_s F(q)(1-G(q))]$ (here the wave vector q is scaled by k_F). We use our analytic form of the local-field factor to calculate the dispersion of the collective modes. Results for the neon and sapphire substrates are shown in figure 7 for various helium film thicknesses and r_s-values. In the thin-film limit ($qd \ll 1$) we observe that the collective mode becomes sound-like in the long-wavelength limit $\omega_{\rm pl}/E_F \simeq sq$, with $s = 2(1 + 1/(z_0^2 + 2z_0))^{1/2}$, where $z_0 = 1/[\sqrt{2}r_s d(\delta_1 + 2\delta_2)(1 - G(0))]$. In the opposite limit of large helium film thickness ($qd \gg 1$), the collective modes assume the form of the typical 2D plasma mode $\omega_{\rm pl}/E_F \simeq (\sqrt{2}r_s(\delta_1 + 2\delta_2)(1 - G(0))q)^{1/2}$. The plasmons enter the particle–hole excitation region at a critical wave vector q_c, determined from $\omega_{\rm pl}(q_c) = q_c^2/2 + q_c$. Beyond q_c the collective modes are heavily damped. The collective modes of diplons with plasmon dispersion and damping properties should in principle be amenable to experimental observation.

The plasmon density of states is defined by $D(E) = \sum_q \delta(E - \omega_{\rm pl}(q))$. Using the analytical expression for the collective mode dispersion $\omega_{\rm pl}(q)$, we find that the density of states is given by

$$D(E) = \frac{m}{\pi}\frac{q_0}{({\rm d}\omega_{\rm pl}/{\rm d}q)\big|_{q_0}} \tag{15}$$

where q_0 is the root of the equation

$$q(1+z)\left[q^2 + \frac{4}{z^2+2z}\right]^{1/2} - E = 0. \tag{16}$$

In figure 8 we display the plasmon density of states as a function of energy for a metallic substrate at $r_s = 10$. The cases for $d = a_B$, $d = 10a_B$, and $d = 100a_B$ are shown by the dotted, dashed, and solid lines, respectively. $D(E)$ exhibits a sharp cut-off beyond a critical value of energy when the corresponding plasmon dispersion curve enters the particle–hole continuum. In the RPA, the plasmons merge with the particle–hole continuum at a higher wave-vector value; thus $D(E)$ would exhibit a broader structure.

4. Discussion and concluding remarks

We have studied the exchange–correlation effects in a system of interacting diplons in the quantum regime. Our results on the static structure factor, pair-correlation function, exchange–correlation energy and plasmon dispersion complement a similar calculation performed by de Freitas *et al* [14] in the classical regime. Including the short-range correlation effects, we obtain significant improvements over the RPA in describing the physical properties of the system. In the STLS treatment of the correlation effects the so-called compressibility sum rule is not satisfied. This may be remedied by introducing another unknown parameter into the analytic form of the proposed local-field factor $G(q)$ as has been demonstrated by Gold [25] for electrons interacting via the bare Coulomb potential. Experimental data on the diplon states are beginning to become available through microwave absorption measurements [9,10,16,17]. Our results on collective mode dispersions and thermodynamic quantities such as compressibility (obtained from the ground-state energy) can be tested in future experiments where the quantum regime is probed systematically with different helium film thicknesses and various substrates. The motion of electrons perpendicular to the helium film surface can also be easily incorporated into the present calculational scheme. For this purpose, the electronic wave function with

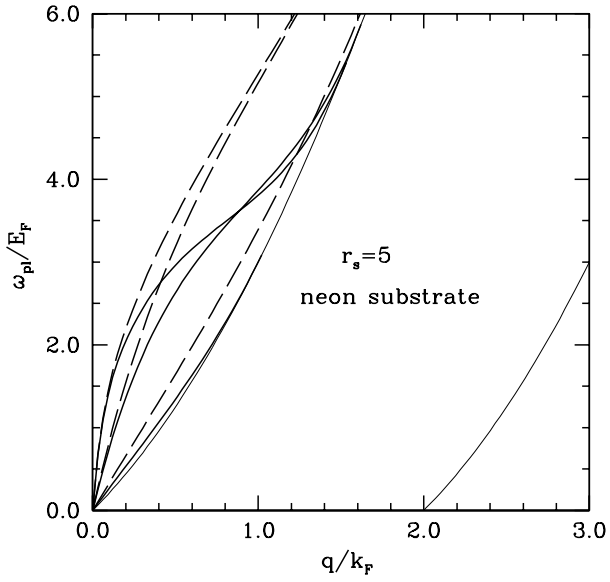

(a)

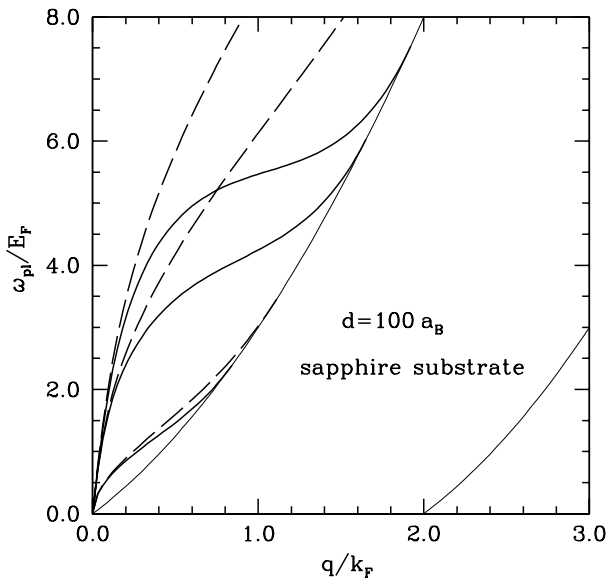

(b)

Figure 7. (a) The plasmon dispersions at $r_s = 5$ for a solid-neon substrate. The thin lines mark the boundaries of the particle–hole continuum. Solid and dashed lines are for the STLS and RPA treatments, respectively. Curves from bottom to top correspond to $d = a_B$, $d = 10a_B$, and $d = 100a_B$, respectively. (b) The plasmon dispersion at $d = 100a_B$ for a sapphire substrate. Curves from bottom to top correspond to $r_s = 1$, $r_s = 10$, and $r_s = 20$, respectively.

finite-width effects and the resulting modification in the interaction potential of the diplons needs to be considered. Our calculations presented here may be checked with the conventional version of the self-consistent-field approach (as opposed to the sum-rule version), and even

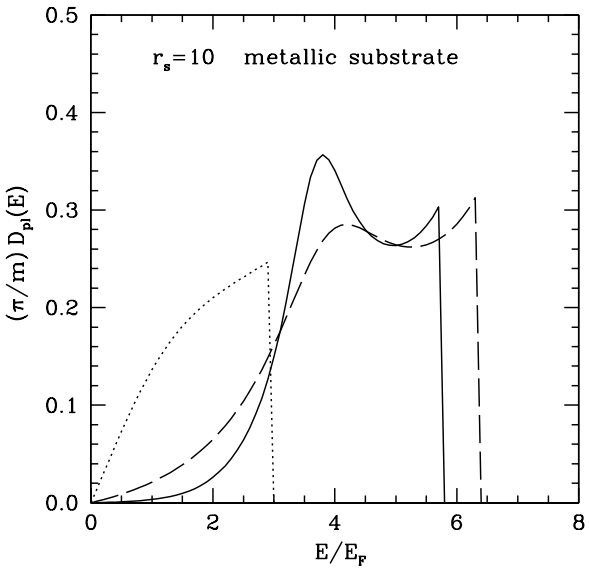

Figure 8. The plasmon density of states at $r_s = 10$ for a metallic substrate ($\epsilon_s = \infty$). The dotted, dashed, and solid lines indicate $d = a_B$, $d = 10a_B$, and $d = 100a_B$, respectively.

better with quantum Monte Carlo simulations, if the experimental results warrant such detailed comparison. The expected Wigner crystal phase at very low densities, the polaronic state of diplons, and the bound-state properties in the presence of impurities could be subjects of further studies.

Acknowledgments

This work was partially supported by the Scientific and Technical Research Council of Turkey (TUBITAK) under Grant No TBAG-1662. We thank Professor I O Kulik and Dr C Bulutay for fruitful discussions.

References

[1] For a recent review see Andrei E Y (ed) 1997 *Two-Dimensional Electron Systems* (Dordrecht: Kluwer)
[2] Grimes C C and Adams G 1979 *Phys. Rev. Lett.* **42** 795
Gallet F, Deville G, Valdes A and Williams F I B 1982 *Phys. Rev. Lett.* **49** 212
[3] Platzman P M and Dykman M I 1999 *Science* **284** 1967
[4] Ma K B and Inkson C J 1978 *J. Phys. C: Solid State Phys.* **11** L411
[5] Peeters F M and Platzman P M 1983 *Phys. Rev. Lett.* **50** 2021
[6] Rino J-P, Studart N and Hipolito O 1984 *Phys. Rev.* B **29** 2584
[7] Peeters F M 1984 *Phys. Rev.* B **30** 159
[8] de Freitas U, Ioriatti L C and Studart N 1987 *J. Phys. C: Solid State Phys.* **20** 5983
[9] Leiderer P 1995 *Z. Phys.* B **98** 303
[10] Gunzler T, Bitnar B, Mistura G, Neser S and Leiderer P 1996 *Surf. Sci.* **341+342** 831
[11] Monarkha Yu P and Kovdrya Yu Z 1982 *Fiz. Nizk. Temp.* **8** 215 (Engl. Transl. 1982 *Sov. J. Low Temp. Phys.* **8** 107)
[12] Monarkha Yu P 1982 *Fiz. Nizk. Temp.* **8** 1133 (Engl. Transl. 1982 *Sov. J. Low Temp. Phys.* **8** 571)
[13] Monarkha Yu P 1979 *Fiz. Nizk. Temp.* **5** 9405 (Engl. Transl. 1979 *Sov. J. Low Temp. Phys.* **5** 447)

[14] de Freitas U, Rino J-P and Studart N 1987 *Lectures on Surface Science: Proceedings of the Fourth Latin-American Symposium (Springer Lectures on Surface Physics)* ed G R Castro and M Cardona (Berlin: Springer) p 177
[15] Cândido L, Rino J-P and Studart N 1998 *Phys. Rev.* B **58** 2844
[16] Karamushko V I, Kovdrya Yu Z, Mende F F and Nikolaenko V A 1982 *Fiz. Nizk. Temp.* **8** 219 (Engl. Transl. 1982 *Sov. J. Low Temp. Phys.* **8** 109)
Kovdrya Yu Z, Mende F F and Nikolaenko V A 1984 *Fiz. Nizk. Temp.* **10** 1129 (Engl. Transl. 1984 *Sov. J. Low Temp. Phys.* **10** 589)
[17] Lehndorff B, Vossloh T, Gunzler T and Dransfeld K 1992 *Surf. Sci.* **263** 674
[18] Dahm A 1995 *Z. Phys.* B **98** 333
[19] Singwi K S, Tosi M P, Land R H and Sjölander A 1968 *Phys. Rev.* **176** 589
[20] Singwi K S and Tosi M P 1981 *Solid State Physics* vol 36 (New York: Academic) p 177
[21] Jena P, Kalia R, Vashishta P and Tosi M P (ed) 1990 *Correlations in Electronic and Atomic Fluids* (Singapore: World Scientific)
[22] Gold A 1992 *Z. Phys.* B **89** 1
[23] Gold A and Calmels L 1993 *Phys. Rev.* B **48** 11 622
[24] Jonson M 1976 *J. Phys. C: Solid State Phys.* **9** 3055
[25] Gold A 1997 *Z. Phys.* B **103** 491